Next-to-leading order QCD corrections to pp→b¯bb¯b + X at the LHC: The quark induced case

Binoth, T ; Greiner, N ; Guffanti, A ; Reuter, J ; Guillet, J P ; Reiter, T

Abstract: The production of two b¯b pairs is a prominent background for Higgs and New Physics searches in various extensions of the Standard Model. We present here the next-to-leading order QCD corrections to the quark induced subprocess using the GOLEM approach for the virtual corrections. We show that our result considerably improves the prediction and conclude that the inclusion of next-to-leading order effects is indispensable for reliable studies of b¯bb¯b observables in hadronic collisions.

DOI: https://doi.org/10.1016/j.physletb.2010.02.010

Originally published at:
Binoth, T; Greiner, N; Guffanti, A; Reuter, J; Guillet, J P; Reiter, T (2010). Next-to-leading order QCD corrections to pp→b¯bb¯b + X at the LHC: The quark induced case. Physics Letters B, 685(4-5):293-296.
DOI: https://doi.org/10.1016/j.physletb.2010.02.010

Next-to-leading order QCD corrections to $pp \to b\bar{b}b\bar{b} + X$ at the LHC: the quark induced case

T. Binoth

School of Physics & Astronomy, The University of Edinburgh, Edinburgh EH9 3JZ, UK

N. Greiner

Institute for Theoretical Physics, Winterthurerstrasse 190, 8057 Zuerich, Switzerland

A. Guffanti, J. Reuter

Department of Physics, University of Freiburg, Hermann-Herder-Str. 3a, D-79104 Freiburg, Germany

J.-Ph. Guillet

LAPTH, 9 Chemin de Bellevue BP 110, 74941 Annecy le Vieux, France

T. Reiter

Nikhef, H225 Science Park 105, 1098 XG Amsterdam, The Netherlands

Abstract

The production of two $b\bar{b}$ pairs is a prominent background for Higgs and New Physics searches in various extensions of the Standard Model. We present here the next-to-leading order QCD corrections to the quark induced subprocess using the `GOLEM` approach for the virtual corrections. We show that our result considerably improves the prediction and conclude that the inclusion of next-to-leading order effects is indispensable for reliable studies of $b\bar{b}b\bar{b}$ observables in hadronic collisions.

Keywords: QCD, higher order corrections, LHC phenomenology

Edinburgh 09/16, FREIBURG-PHENO-09-05, LAPTH-1358/09, Nikhef 2009-026, ZU-TH 16/09

1. Introduction

With the LHC data taking on the horizon, the quest for precise predictions for multi-parton processes becomes more and more pressing. The confirmation of the Higgs sector of the Standard Model (SM) and the exploration of the TeV scale with respect to New Physics will ultimately

Email addresses: `thomas.binoth@ed.ac.uk` (T. Binoth), `greiner@physik.unizh.ch` (N. Greiner), `alberto.guffanti@physik.uni-freiburg.de`, `reuter@physik.uni-freiburg.de` (A. Guffanti, J. Reuter), `guillet@lapp.in2p3.fr` (J.-Ph. Guillet), `thomasr@nikhef.nl` (T. Reiter)

depend on a very detailed understanding of signal and background processes [1, 2, 3, 4]. Especially in hadronic collisions, scale uncertainties lead to a strong logarithmic dependence if only leading order (LO) perturbation theory is applied. Whereas the inclusion of next-to-leading order (NLO) QCD effects is relatively straightforward for simple kinematic situations already for four parton final states the number of results is very limited. The complexity of next-to-leading order computations with many external partons are many-fold. It is not only necessary to provide a numerically stable implementation of the ultra-violet (UV) renormalised one-loop amplitude, one also has to combine the different parts of the computation such that infrared (IR) divergences are compensated between virtual and real emission corrections. After IR cancellations the integrands are finite and a stable integration over phase space can be achieved. In all respects a lot of progress has happened in the last few years which point towards automated approaches concerning the one-loop amplitudes [5, 6, 7, 8, 9, 10, 11, 12, 13, 14, 15, 16, 17] and IR subtraction modules [18, 19, 20, 21, 22, 23] which can be combined with publicly available Monte-Carlo tools [24, 25, 26, 27, 28, 29, 30].

Recent achievements are the evaluation of the order α_s corrections to $pp \to b\bar{b}t\bar{t}$ [31, 32, 33] and $pp \to Wjjj$ [34, 35, 36, 37]. In both cases the inclusion of higher order effects leads to the expected improvement in predictability of corresponding production rates which is of importance for Higgs and New Physics searches.

In this paper we present a result of similar complexity which is relevant in the context of Higgs searches in the Minimal Supersymmetric Standard Model (MSSM) and two Higgs doublet extensions of the SM, where five scalar Higgs bosons are present. To scan and explore the parameter space in these models Higgs pair production is a relevant handle. As light Higgs bosons prefer to decay into b-quarks in large parts of parameter space, experimental studies are so far strongly affected by the uncertainty of the Standard Model backgrounds, especially $pp \to b\bar{b}b\bar{b}$, see for example Ref. [38]. Although mainly motivated by supersymmetry, the four-b final state also allows the study of other interesting beyond Standard Model (BSM) scenarios such as hidden valley models, where decays of hadrons of an additional confining gauge group can produce high multiplicities of $b\bar{b}$ pairs [2, 39]. This is the reason why the $pp \to b\bar{b}b\bar{b}$ process was added to the experimenters wish-list of relevant next-to-leading order computations [2].

For the evaluation of the process $pp \to b\bar{b}b\bar{b}$ two partonic initial states contribute at tree level: $gg \to b\bar{b}b\bar{b}$ and $q\bar{q} \to b\bar{b}b\bar{b}$. In this article we present the next-to-leading order QCD results for the quark induced process. Our calculation is based on the `GOLEM` approach for one-loop amplitudes [8, 40, 41, 43] which has already been applied in amplitude computations of various complexity [44, 45, 46, 47]. The IR divergences are treated using the Catani-Seymour dipole subtraction method [49] implemented in `MadDipole` [20]. For the evaluation of tree amplitude contributions the matrix element generators `Madgraph/MadEvent` [24, 25] and `Whizard` [27, 48] are used. In the latter the relevant dipole subtraction terms have been included, too.

In the next section we will briefly sketch how our result is obtained and in section 3 numerical results are presented. Section 4 resumes the paper.

2. Calculation

At leading order two topologies contribute to the amplitude $q\bar{q} \to b\bar{b}b\bar{b}$, see Fig. (1). As the parton distribution functions for the b-quarks are very small we only consider the cases $q = u, d, s, c$. We treat the b-quarks as massless which is a very good approximation for LHC kinematics and cuts as long as the b-quarks can be detected and are sufficiently separated in phase space. Effects of the heavy top quark are neglected altogether as they are numerically not important.

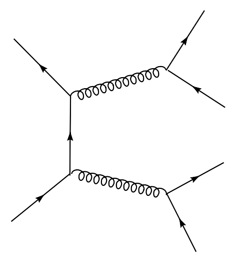

Figure 1: Six-quark topologies which contribute to the leading order amplitude $q\bar{q} \to b\bar{b}b\bar{b}$.

2.1. Virtual corrections

The evaluation of the virtual corrections is the technically most challenging part of the calculation. Our approach is based on the Feynman diagrammatic representation of the amplitude. The most complicated topologies are of pentagon and hexagon type as shown in Fig. (2). We evaluated all Feynman diagrams in two independent ways using the 't Hooft-Veltman scheme. What is common to both methods is the projection onto different helicity and colour structures. One strategy (1) is to convert the Feynman diagrams to a form factor representation and to evaluate these and the resulting objects numerically. In this case we use Feynman diagram representations generated with `QGRAF` [50]. `FORM` [51] is used to map the helicity amplitudes to a tensor form factor representation as defined in [8, 16, 53]. The latter is exported to `Fortran95` code such that it can be linked to the form factor library `golem95` [42]. For the code generation we have developed a dedicated optimisation tool which can also be used for other purposes [54]. The other strategy (2) is to perform a symbolic tensor reduction down to genuine scalar integrals. Here we use `FeynArts` and `FeynCalc` [52] to generate the amplitudes. The tensor integrals are reduced symbolically to scalar integrals also using the formalism described in [8]. As a scalar integral basis we choose two- and three-point functions in $D = 4 - 2\epsilon$-dimensions and four-point functions in 6 dimensions. In this way the extraction of infrared and ultraviolet poles is very transparent. In both strategies the reduction of the five-point tensor integrals is done without introducing inverse Gram-determinants.

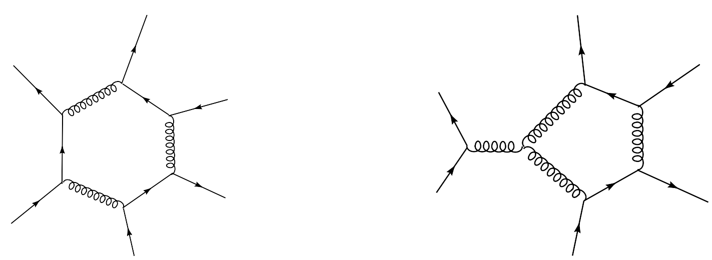

Figure 2: Pentagon and hexagon one-loop topologies which contribute to the virtual corrections to order $\mathcal{O}(\alpha_s^3)$.

Without UV counterterms and IR subtraction terms one has non-vanishing coefficients for double and single poles in $1/\epsilon$. Adding in the UV counterterm and the Catani-Seymour IR insertion operator, $I(\epsilon)$ [49], results in the numerical cancellation of the pole part. This by itself is a stringent check on the algebra.

All Feynman diagrams are thus evaluated in two completely independent manners. Together with the cancellation of UV/IR poles and the test of symmetry properties of helicity amplitudes the correctness of the virtual amplitudes is well checked.

2.2. Real emission corrections

Apart from the one-loop corrections we have to consider processes with an extra parton in the final state. In this paper we restrict ourselves to $q\bar{q}$ initial states. Further we are only interested in observables with four well separated b-jets where the b-quarks can be tagged. The relevant amplitude is thus $q\bar{q} \to b\bar{b}b\bar{b}g$. If the extra gluon is soft and/or collinear infra-red divergences are treated by using the dipole subtraction method of Catani-Seymour [49]. In our case 30 dipole subtraction terms are needed. In processes with so many dipoles the efficiency of the integration over phase space can be improved considerably if the dipole terms are only subtracted in restricted regions. In the approach of [55] a slicing parameter α controls the size of phase space where the subtraction terms are included. This method is adopted here. Eventually the results must not depend on the slicing parameter α. We have carefully checked that this is indeed the case.

For the evaluation of all tree like contributions of our process, i.e. the LO contribution and the real emission corrections including dipole subtraction, we use adapted versions of the tree level event generators `Madgraph/MadEvent` [24, 25] and `Whizard` [27, 48]. For the IR subtractions we use `MadDipole` [20] supplemented by integrated dipole contributions. Again we have two fully independent implementations which should guarantee the correctness of the result.

3. Results

In this section we provide our prediction for the quark induced four b-quark production rate at next-to-leading order QCD for the LHC. We use $\sqrt{s} = 14$ TeV as center-of-mass energy for all results. To define a $b\bar{b}b\bar{b}$ event we use the following strategy.

1.) First we apply a jet algorithm to identify the phase space region where the b-quarks can be separated from the extra gluon jet by applying the k_T jet algorithm as explained in [56]. If a gluon is merged with a b-quark we obtain an effective b-quark with a momentum $\tilde{p}_b = p_g + p_b$.

2.) We apply separation cuts on the four resolved b-quarks which are defined by the transverse momenta, rapidities and separation parameters as

$$\begin{aligned} p_T(b_j) &> 30 \text{ GeV} \\ |\eta(b_j)| &< 2.5 \\ \Delta R(b_i, b_j) &> 0.8 \quad . \end{aligned} \tag{1}$$

The separation cut is defined in terms of the azimuthal and rapidity differences of the (effectively) observed b-quarks, i.e. $\Delta R(b_i, b_j) = \sqrt{(\phi_i - \phi_j)^2 + (\eta_i - \eta_j)^2}$. Note that in the case of an unresolved gluon/b system the effective momentum $\tilde{p}_b$ is used to test the cut conditions. We use the CTEQ6M parton distribution functions [57] with 2-loop running for α_s for both the LO and NLO order cross section evaluations.

In Fig. 3 we show the renormalisation scale (μ_R) dependence of our LO and NLO results. We vary the renormalisation scale around a standard scale μ_0 which we define as the sum of the squared transverse b-quark momenta, $\mu_0 = \sqrt{\sum_j p_T^2(b_j)}$. The factorisation scale is fixed to $\mu_F = 100$ GeV. As not all initial states are included yet we postpone the study of the μ_F dependence to a forthcoming paper. As expected the LO result shows a strong monotonous dependence on

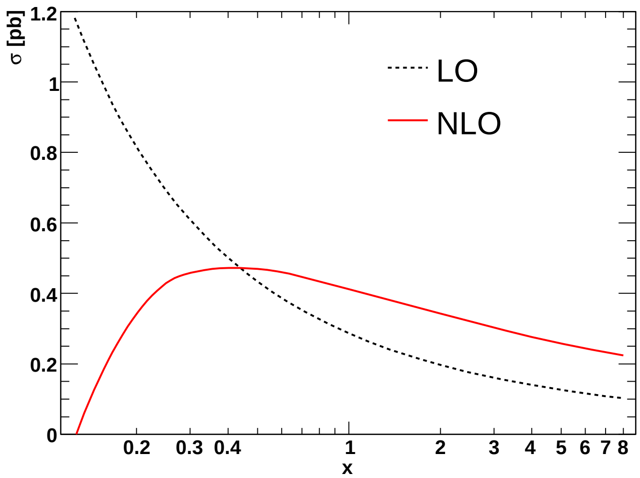

Figure 3: The dependence of the LO and NLO prediction of $pp(q\bar{q}) \to b\bar{b}b\bar{b} + X$ at the LHC ($\sqrt{s} = 14$ TeV) on the renormalisation scale $\mu_R = x\mu_0$ with $\mu_0 = \sqrt{\sum_j p_T^2(b_j)}$. The factorisation scale is fixed to $\mu_F = 100$ GeV.

$x = \mu_R/\mu_0$. Inclusion of the NLO corrections leads to a cancellation of the leading logarithmic dependence such that the NLO result has now a plateau for a value around $x \sim 1/2$, where the prediction shows the desired stability under scale variation.

As a reference we provide cross section values for four scale choices in Tab. 1.

μ_R	σ_{LO} [fb]	σ_{NLO} [fb]
$2\mu_0$	197.1	342.7
μ_0	286.8	413.8
$\mu_0/2$	434.0	463.0
$\mu_0/4$	692.4	434.0

Table 1: Total LO and NLO cross sections for different renormalisation scale choices. As a standard scale we use $\mu_0 = \sqrt{\sum_j p_T^2(b_j)}$. The factorisation scale is set to $\mu_F = 100$ GeV. The precise definition of the four-b observable is given in the text. The error on all these numbers is estimated to be well below 1%.

Finally, we compare the LO and NLO prediction of the invariant mass distribution of the leading b-pair in Fig 4. This invariant mass distribution is defined by the leading and sub-leading b ($\bar{b}$) quark, i.e. we choose the two quarks with the largest p_T and evaluate the invariant mass of this system. We define an uncertainty band by varying the renormalisation scale μ_R around the scale between $\mu_0/4$ and $2\mu_0$, where again $\mu_0 = \sqrt{\sum_j p_T^2(b_j)}$. This asymmetric scale choice is motivated by the asymmetric shape of the NLO μ_R dependence, see Fig. 3. For the scale $\mu_R = \mu_0/2$ the LO and NLO distributions look very similar which is indicated by the full (NLO) and dashed (LO) line in Fig. 4. This is consistent with Fig. 3 as for this value the inclusive cross sections almost

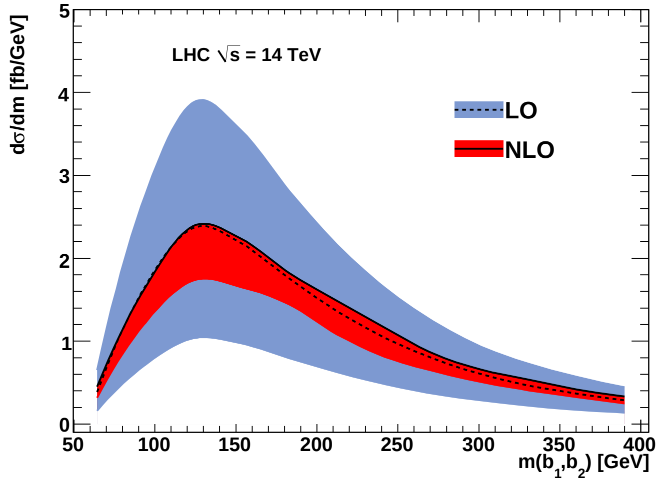

Figure 4: Invariant mass (m_{bb}) distribution of the two leading b-quarks (see text). The LO/NLO bands are obtained by varying the renormalisation scale μ_R between $\mu_0/4$ and $2\mu_0$ with $\mu_0 = \sqrt{\sum_j p_T^2(b_j)}$. The full (dashed) line shows the NLO (LO) prediction for the value $\mu_R = \mu_0/2$.

coincide. The importance of the higher order terms is evident from the uncertainty band which is considerably reduced after inclusion of the NLO QCD corrections.

4. Conclusion

In this letter we have presented the next-to-leading order QCD prediction for the quark induced four-b cross section at the LHC. It is the first part of a complete NLO QCD evaluation of $pp \to b\bar{b}b\bar{b} + X$. This final state is an important background for BSM Higgs searches at the LHC as it is a prominent final state for Higgs pair production in large regions of parameter space.

From the technical point of view we have provided another example for the Feynman diagrammatic approach being well capable to compute one-loop processes of such a complexity. We have used the `GOLEM` method implemented in a highly automated framework such that further results can be obtained with the same set-up. Two independent evaluation strategies guarantee the validity of the result. For the tree-level amplitudes we use `Madgraph/MadEvent` in combination with `MadDipole` and `Whizard`. For the latter the relevant dipole terms have been added. We observe that the evaluation time for any observable is dominated by the real emission part of the calculation. Future improvements can be expected by phase-space parametrisations which are adapted to a given IR subtraction method.

We have shown for the quark induced case that the inclusion of the order α_s corrections leads to a significant improvement of predictions for four b-observables at the LHC as the renormalisation scale dependence is considerably reduced. The same can be expected for the the gluon induced case which is under construction using the same methods.

Acknowledgements

We would like to thank Thomas Gehrmann for interesting and useful discussions. T.B. thanks the University of Freiburg and Nikhef in Amsterdam, where parts of this work have been done, for their hospitality. T.B. is supported in parts by STFC, SUPA and the IPPP Durham. N.G. thanks the Universities Edinburgh, Freiburg and the IPPP in Durham for supporting various visits where work on the project was done. N.G. was supported by the Swiss National Science Foundation (SNF) under contract 200020-126691. T.R. thanks the University of Zuerich and J.R. wants to thank the Aspen and Les Houches Centers of Physics for their hospitality. J.R. was partially supported by the Baden-Wuerttemberg Ministry of Science and Culture. Part of the computations were done on the ECDF cluster at the University of Edinburgh.

[1] N. E. Adam *et al.*, hep-ph/0803.1154.

[2] Z. Bern *et al.* [NLO Multileg Working Group], hep-ph/0803.0494.

[3] C. Buttar *et al.*, hep-ph/0604120.

[4] J. M. Campbell, J. W. Huston and W. J. Stirling, Rept. Prog. Phys. **70** (2007) 89 [hep-ph/0611148].

[5] T. Binoth, hep-ph/0903.1876.

[6] C. F. Berger *et al.*, Phys. Rev. D **78**, 036003 (2008) [hep-ph/0803.4180].

[7] Z. Bern, L. J. Dixon and D. A. Kosower, Annals Phys. **322** (2007) 1587 [hep-ph/0704.2798].

[8] T. Binoth, J. P. Guillet, G. Heinrich, E. Pilon and C. Schubert, JHEP **0510** (2005) 015 [hep-ph/0504267].

[9] R. Britto, B. Feng and P. Mastrolia, Phys. Rev. D **78**, 025031 (2008) [hep-ph/0803.1989].

[10] A. Denner and S. Dittmaier, Nucl. Phys. B **734** (2006) 62 [hep-ph/0509141].

[11] T. Diakonidis, J. Fleischer, J. Gluza, K. Kajda, T. Riemann and J. B. Tausk, Phys. Rev. D **80** (2009) 036003 [hep-ph/0812.2134].

[12] W. T. Giele and G. Zanderighi, JHEP **0806**, 038 (2008) [hep-ph/0805.2152].

[13] T. Hahn, arXiv:0901.1528 .

[14] A. Lazopoulos, hep-ph/0812.2998.

[15] G. Ossola, C. G. Papadopoulos and R. Pittau, Nucl. Phys. B **763**, 147 (2007) [hep-ph/0609007].

[16] T. Reiter, hep-ph/0903.0947.

[17] J. C. Winter and W. T. Giele, hep-ph/0902.0094.

[18] T. Gleisberg and F. Krauss, Eur. Phys. J. C **53**, 501 (2008) [hep-ph/0709.2881].

[19] M. H. Seymour and C. Tevlin, hep-ph/0803.2231.

[20] R. Frederix, T. Gehrmann and N. Greiner, JHEP **0809**, 122 (2008) [hep-ph/0808.2128].

[21] K. Hasegawa, S. Moch and P. Uwer, Nucl. Phys. Proc. Suppl. **186**, 86 (2009).

[22] M. Czakon, C. G. Papadopoulos and M. Worek, JHEP **0908**, 085 (2009) [hep-ph/0905.0883].

[23] R. Frederix, S. Frixione, F. Maltoni and T. Stelzer, hep-ph/0908.4272.

[24] T. Stelzer and W. F. Long, Comput. Phys. Commun. **81**, 357 (1994) [hep-ph/hep-ph/9401258].

[25] F. Maltoni and T. Stelzer, JHEP **0302**, 027 (2003) [hep-ph/hep-ph/0208156].

[26] A. Cafarella, C. G. Papadopoulos and M. Worek, Comput. Phys. Commun. **180**, 1941 (2009) [hep-ph/0710.2427].

[27] W. Kilian, T. Ohl and J. Reuter, hep-ph/0708.4233.

[28] T. Sjostrand, S. Mrenna and P. Skands, JHEP **0605**, 026 (2006) [hep-ph/0603175].

[29] M. Bahr *et al.*, Eur. Phys. J. C **58**, 639 (2008) [hep-ph/0803.0883].

[30] T. Gleisberg, S. Hoche, F. Krauss, M. Schonherr, S. Schumann, F. Siegert and J. Winter, JHEP **0902**, 007 (2009) [hep-ph/0811.4622].

[31] A. Bredenstein, A. Denner, S. Dittmaier and S. Pozzorini, JHEP **0808**, 108 (2008) [hep-ph/0807.1248].

[32] A. Bredenstein, A. Denner, S. Dittmaier and S. Pozzorini, Phys. Rev. Lett. **103**, 012002 (2009) [hep-ph/0905.0110].

[33] G. Bevilacqua, M. Czakon, C. G. Papadopoulos, R. Pittau and M. Worek, JHEP **0909**, 109 (2009) [hep-ph/0907.4723].

[34] C. F. Berger *et al.*, hep-ph/0907.1984.

[35] C. F. Berger *et al.*, Phys. Rev. Lett. **102**, 222001 (2009) [hep-ph/0902.2760].

[36] R. K. Ellis, K. Melnikov and G. Zanderighi, hep-ph/0906.1445.

[37] R. K. Ellis, K. Melnikov and G. Zanderighi, JHEP **0904** (2009) 077 [hep-ph/0901.4101].

[38] R. Lafaye, D. J. Miller, M. Muhlleitner and S. Moretti, hep-ph/0002238.

[39] W. Krolikowski, hep-ph/0803.2977.

[40] T. Binoth *et al.*, hep-ph/0807.0605.

[41] T. Binoth, J. P. Guillet and G. Heinrich, Nucl. Phys. B **572** (2000) 361 [hep-ph/9911342].

[42] T. Binoth, J. P. Guillet, G. Heinrich, E. Pilon and T. Reiter, Comput. Phys. Commun. **180**, 2317 (2009) [hep-ph/0810.0992].

[43] T. Binoth, J. P. Guillet and G. Heinrich, JHEP **0702**, 013 (2007) [hep-ph/0609054].

[44] T. Binoth, M. Ciccolini, N. Kauer and M. Kramer, JHEP **0503**, 065 (2005) [hep-ph/0503094].

[45] T. Binoth, S. Karg, N. Kauer and R. Ruckl, Phys. Rev. D **74** (2006) 113008 [hep-ph/0608057].

[46] J. R. Andersen, T. Binoth, G. Heinrich and J. M. Smillie, JHEP **0802**, 057 (2008) [hep-ph:0709.3513].

[47] T. Binoth, G. Heinrich, T. Gehrmann and P. Mastrolia, Phys. Lett. B **649** (2007) 422 [hep-ph/0703311].

[48] M. Moretti, T. Ohl and J. Reuter, hep-ph/0102195.

[49] S. Catani and M. H. Seymour, Nucl. Phys. B **485**, 291 (1997) [Erratum-ibid. B **510**, 503 (1998)] [hep-ph/9605323].

[50] P. Nogueira, J. Comput. Phys. **105**, 279 (1993).

[51] J. A. M. Vermaseren, arXiv:math-ph/0010025.

[52] T. Hahn and M. Perez-Victoria, Comput. Phys. Commun. **118**, 153 (1999) [hep-ph/9807565].

[53] T. Reiter, hep-ph/0903.4648.

[54] T. Reiter, hep-ph/0907.3714.

[55] Z. Nagy and Z. Trocsanyi, Phys. Lett. B **634** (2006) 498 [hep-ph/0511328].

[56] G. C. Blazey *et al.*, hep-ex/0005012.

[57] J. Pumplin, D. R. Stump, J. Huston, H. L. Lai, P. M. Nadolsky and W. K. Tung, JHEP **0207** (2002) 012 [hep-ph/0201195].